Synthesis of $MnMoO_4$ as High Capacity Anode Material for Li Secondary Battery

Sung-Soo Kim, Seiichiro Ogura, Hiromasa Ikuta, Yoshiharu Uchimoto, and Masataka Wakihara*
Department of Applied Chemistry, Graduate School of Science and Engineering, Tokyo Institute of Technology, 2-12-1 Ookayama, Meguro-ku, Tokyo 152-8552

(Received May 9, 2001; CL-010423)

$MnMoO_4$(*C2/m*) as a new anode material for Li secondary battery has been synthesized by a conventional solid state reaction method and its electrochemical properties have been investigated. Mn *L*-edge XANES indicates that the energy of the main peak of $MnMoO_4$ is close to that of $MnCO_3$ (Mn^{2+}). Mo *L*-edge XANES shows that the oxidation state of Mo in $MnMoO_4$ is +6. The reversible amount of Li insertion/removal in $MnMoO_4$ anode during the first cycle was about 1000 Ah/kg. Capacity variation with the current density shows that the rate capability of $MnMoO_4$ is better than that of graphite.

The Li-ion rechargeable batteries are considered as the most suitable power sources for portable electronic devices due to their high capacity and energy density. The graphite anode material commonly used in Li-ion rechargeable batteries suffers from small capacity per unit weight (about 350 Ah/kg) and/or per unit volume due to its low density. To overcome these disadvantages, considerable amounts of attempts have been made to find out alternative anode materials, including metal oxides (MO; M = Co, Ni, Fe),[1] tin-based material,[2] vanadium-based oxide materials,[3,4] in place of graphite anodes. Recently, several researchers have described the low potential Li-insertion behavior in vanadium-based oxides such as RVO_4 (R = In, Cr, Fe, Al, Y)[3] and MnV_2O_6[4]. Molybdenum oxides should be attractive as anode materials, because they also have various oxidation states like vanadium. Previously, the molybdenum oxide MoO_2 as an anode material of a lithium secondary battery was proposed by Auborn[5] more than 10 years ago, but their study was limited by experimental conditions such as poor stability of the electrolyte at low potential.

In this study, we synthesized molybdenum-based oxide $MnMoO_4$ as a new anode material and described the lithium insertion/removal behavior at low potential cycle property. The XRD measurement and X-ray absorption study of Mn and Mo *L*-edge have provided insights on the structure and oxidation state of the transition metals.

$MnMoO_4$ powder sample was prepared by conventional solid reaction method. Starting materials used were $MnCO_3$ (99.9% Soekawa Chemicals) and MoO_3 (99.9% Soekawa Chemicals). These reagents were mixed with stoichiometric ratio in an agate mortar and the mixture was heat-treated at 600 °C for 24 h in air atmosphere. The phase identification of prepared samples was carried out by powder X-ray diffractometry using Rigaku RINT2500V with Cu Kα radiation. The samples for electrochemical measurements were prepared by mixing crystalline $MnMoO_4$, acetylene black as conductive agent and polytetraflouroethylene (PTFE) binder (55–40–5 wt%) in an agate mortar and made in the form of film. The film was then cut into a disk form. Cells were fabricated by coupling this disk with lithium foil as counter electrode using microporous polypropylene film as separator. 1M $LiClO_4$ dissolved in ethylene carbonate (EC)/diethlylene carbonate (DEC) (vol ratio = 1:1) was used as the electrolyte. The electrochemical measurement was carried out galvanostatically at various current densities at room temperature in a glove box under argon atmosphere. The cut-off voltage was set at 0.0 and 2.0 V vs Li/Li^+. Mo L_{23}-edge X-ray absorption near edge structure (XANES) was measured on BL7A at UVSOR (Okazaki, Japan) with a ring energy of 750 MeV and a stored current of 70–220 mA in a mode of total electron yields. The KTP double crystal monochromator was used. The absolute energy scale was calibrated by using literature value of Mo L_{23}-edge in MoO_3. Mn L_{23}-edge XANES was measured on BL8B1 beam line at UVSOR (Okazaki, Japan) with ring energy of 750 MeV in a mode of total electron yield at room temperature.

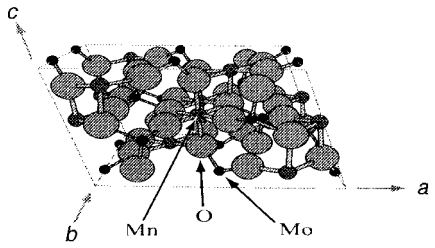

Figure 1. Schematic diagram of α-$MnMoO_4$ structure

Crystal structure of the synthesized powder was examined by X-ray diffractometry analysis. The well-defined XRD pattern obtained confirms that the prepared compound is $MnMoO_4$ without any impurity phases. The prepared sample can be indexed completely by JCPDS data (card number 27-1280). The lattice constants of prepared $MnMoO_4$ are 10.47 Å (*a*), 9.53 Å (*b*) and 7.15 Å (*c*) which agree fairly well with JCPDS data and previous report[6]. This structure has been known as α-$MnMoO_4$, which is composed of strongly distorted octahedral coordinated Mn and slightly distorted tetrahedral coordinated Mo by oxygen[6]. Figure 1 depicts the crystal structure of α-$MnMoO_4$. The two crystallographically independent Mn atoms share the edge of octahedra. There is tunnel-like space surrounded by MoO_4 tetrahedra and MnO_6 octahedra along *b*-axes which can be considered as diffusion path during Li insertion/removal. XANES results were shown in Figure 2 with reference materials having various oxidation states. The absorption shown in Figure 2 around 640–645 eV is $2p_{3/2}$ (L_3) edge. In Figure 2(a), the energy of a main peak of $MnMoO_4$ is close to that of $MnCO_3$. This result indicates Mn exists as Mn^{2+} in $MnMoO_4$. Mo L_{23}-edge XANES spectra of $MnMoO_4$ and MoO_3 presented in the Figure 2(b) illustrate that the valence of Mo in $MnMoO_4$ should be +6. Furthermore, the spectra of Mo *L*-edge XANES of $MnMoO_4$ and MoO_3, which involves the transitions from the 2p core levels into the empty 4d orbital, show separation of two peaks clearly. In octahedral coordinated metal, the d-orbitals split into triply degenerate t_{2g} and doubly degenerate

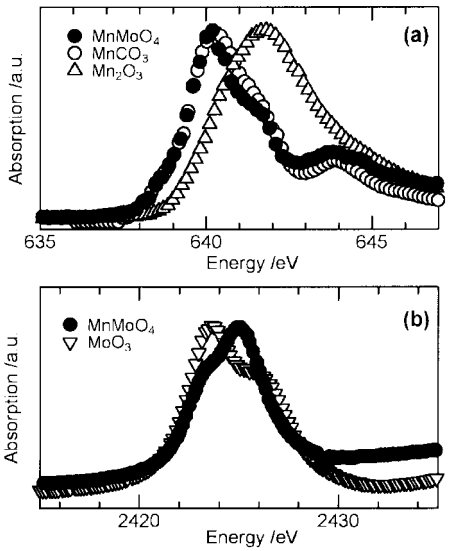

Figure 2. (a) Mn *L*-edge XANES spectrum of $MnMoO_4$ and various compounds as reference. (b)Mo *L*-edge XANES spectrum of $MnMoO_4$ and MoO_3.

e_g orbitals, whereas, in tetrahedral coordination, triply degenerate t_2 orbitals lie higher in energy than doubly degenerate e orbitals. The Mo atoms in MoO_3 are in octahedral environment, and Figure 2(b) indicates the typical 4d splitting in two sets of e_g and t_{2g} symmetry. On the other hand, the Mo atoms in $MnMoO_4$ are in a tetrahedral environment, and Figure 2(b) shows ligand field splitting parameter (Δ_T: energy difference of t_2 and e) is about 1.6 eV. The difference of d-orbital splitting between tetrahedral and octahedral coordination has been reported on several molybdates previously[7].

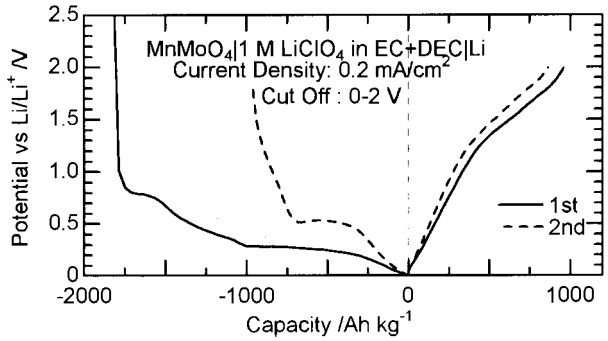

Figure 3. Charge–discharge profile of $MnMoO_4$/Li test cell.

The charge–discharge profiles obtained are shown in Figure 3. The initial charge capacity was about 1800 Ah/kg and it shows the capacity about 1000 Ah/kg reversibly in subsequent discharge process. The reversible capacity of about 1000 Ah/kg is almost 3 times larger than that of graphite (~350 Ah/kg) which is used as anode material for commercial Li-ion secondary battery. During the first charge, the lithium intercalation process exhibited a plateau around 0.8 V vs Li/Li^+ which is not observed in the following cycles. The difference between the first and the second charge profile is also indicative of the two different mechanisms operating in the lithium insertion process. Although further investigation must be needed to understand the precise reaction mechanism, it can be assumed that the anion participation in Li accommodation by the hybridization of O 2p and Mo 4d orbitals con-

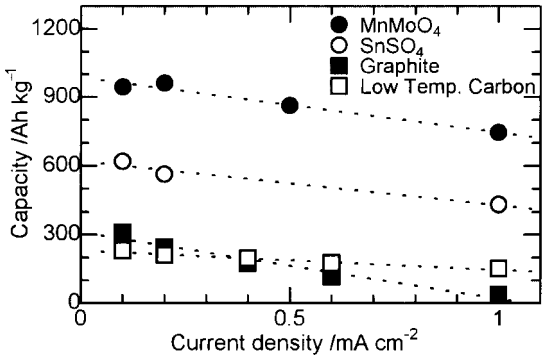

Figure 4. The discharge capacity variations of $MnMoO_4$ and the other reference materials with current density.

tributes to high capacity. Figure 4 shows the capacity variation with the current density of $MnMoO_4$ together with other anode materials. Each value in the figure corresponds to the discharge capacity of the first cycle. From these results, $MnMoO_4$ shows rather high rate capability compared with the other anode material. The cycling behavior over several tens of cycles is shown in Figure 5. It shows moderate capacity fading with cycling. Even after 25 cycles, the capacity shows more than 400 Ah/kg.

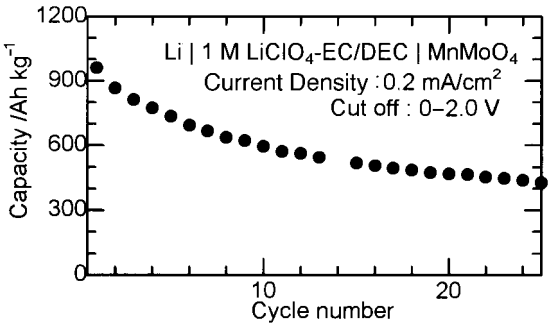

Figure 5. The discharge capacity variation with cycle number of $MnMoO_4$/Li test cell.

In conclusion, we synthesized $MnMoO_4$ as a novel anode material for lithium secondary batteries. The initial capacity realized during the first lithium insertion was 1800 Ah/kg and reversible capacity in consequent cycle was about 1000 Ah/kg. Through the results of capacity variation in various current densities the present $MnMoO_4$ shows better rate capability than other anode materials.

References and Notes

1 P. Poizot, S. Laruelle, S. Grugeon, L. Dupont, and J-M. Tarascon, *Nature*, **407**, 496 (2000).
2 Y. Idota, T. Kubota, A. Matsufuji, Y. Maekawa, and T. Miyasaka, *Science*, **276**, 1395 (1997).
3 S. Denis, E. Baudrin, M. Touboul, and J-M. Tarascon, *J. Electrochem. Soc.*, **144**, 3886 (1997).
4 S-. S. Kim, H. Ikuta, and M. Wakihara, *Solid State Ionics*, **139**, 57 (2001).
5 J. J. Auborn and Y. L. Baberio, *J. Electrochem. Soc.*, **134**, 638 (1987).
6 A. Clearfiled, A. Moini, and P. R. Rudolf, *Inorg. Chem.*, **24**, 4606 (1985).
7 J. A. Rodriguez, J. C. Hanson, S. Chaturvedi, A. Maiti, and J. L. Brito, *J. Phys. Chem. B*, **104**, 8145 (2000).
8 M. Nagayama, T. Morita, H. Ikuta, M. Wakihara, M. Takano, and S. Kawasaki, *Solid State Ionics*, **106**, 33 (1998).